Research Article

Author for correspondence:
Naveen Gupta, Lovely Professional University, Physics, Delhi Highway, Phagwada, Punjab, 144411, E-mail: naveens222@rediffmail.com

Second harmonic generation of *q*-Gaussian laser beam in plasma channel created by ignitor heater technique

Naveen Gupta

School of Physical and Chemical Sciences, Lovely Professional University, Phagwara, India

Abstract

This paper presents a scheme for second harmonic generation (SHG) of *q*-Gaussian laser beam in plasma channel created by ignitor heater technique. The ignitor beam creates plasma by tunnel ionization of air. The heater beam heats the plasma electrons and establishes a parabolic density profile. The third beam (*q*-Gaussian beam) is guided in this plasma channel under the combined effects of density nonuniformity of the plasma channel and relativistic mass nonlinearity of the plasma electrons. The propagation of *q*-Gaussian laser beam through the plasma channel excites an electron plasma wave at pump frequency that interacts with the incident laser beam to produce its second harmonics. The formulation is based on finding the numerical solution of the nonlinear Schrodinger wave equation for the fields of the incident laser beams with the help of moment theory approach. Particular emphasis is put on dynamical variations of the spot size of the laser beams and conversion efficiency of the second harmonics with distance of propagation.

Introduction

High intensity laser guiding over lengths greater than centimeters is one of the key issues for future laser-plasma accelerators (Tajima and Dawson, 1979; Modena *et al.*, 2002) and other applications such as X-ray lasers (Faenov *et al.*, 2007), harmonic generation (Malka *et al.*, 1997; Gupta and Singh, 2016), and so on. In laser plasma accelerators (Esarey *et al.*, 2009), the pondero intense laser beam drives a plasma wave that can accelerate particles to extremely high energies. The performance of such accelerators can be greatly enhanced by guiding the drive laser beam, which must be at or above an intensity 10^{18} W/cm^2 to produce high accelerating fields. To reach GeV energies, cm-scale acceleration distances are required. However, in the absence of an optical guiding mechanism, diffraction broadening of the laser beam limits the interaction length only up to a Rayleigh length. Hence, guiding of laser beams is essential to enhance the performance of the laser-driven accelerators. By maintaining the laser intensity over several Rayleigh lengths, controlled guiding can allow efficient production of a long, high gradient wake structures. In conventional optics, one can obviate the diffraction broadening of the laser beams by using optical fibers. In applications involving laser–plasma interactions laser beams having intensities over 10^{18} W/cm^2 are being used. However, glass fibers undergo ionization induced damages only at 10^{12} W/cm^2. But by using plasma channels, that are impervious to optical damage, as the guiding medium, such limitation could be significantly surpassed. Plasma channels, thus offer a practical solution to the problem of extending the interaction lengths beyond the limit set by geometric diffraction (Esarey *et al.*, 1997).

Plasma channels have been created in the laboratory by a variety of methods: (1) Passing a long laser pulse through an optic to create a line focus in a gas, which ionizes and heats the gas, creating a radially expanding hydrodynamic shock (Clark and Milchberg, 1997; Johnson *et al.*, 2001) (2) using a slow capillary discharge to control the plasma density profile (Ehrlich *et al.*, 1996) (3) using the ponderomotive force of an intense, relativistically self-guided laser pulse in a plasma which creates a channel in its wake (Young and Bolton, 1996; Clayton *et al.*, 1998).

The principle behind plasma channel guiding is that a plasma column that has a radial density profile with an on-axis minimum can, through the dependence of refractive index on plasma density, acts as lens for the laser beam. Guiding over long distances is possible due to the balance between the inward bending of the light rays through the refractive index gradient and outward expansion through geometric diffraction. To guide highly intense laser beams, plasma channels must be produced in deeply ionized gases, where the density profile cannot be changed by the guided beam through further ionization. An increase in density on axis would lead to ionization-induced refraction and hence negate the guiding (Leemans *et al.*, 1992). To meet these requirements Volfbeyn *et al.* (1999) developed a novel technique which, rather than utilizing a single laser beam for ionization and heating, makes use of two laser beams. The physics of guiding the laser beam is as follows: The ignitor beam creates plasma

by tunnel ionization of ambient gas. The heater beam heats the existing plasma and thus creates a concave parabolic electron density profile so that the plasma density becomes minimum on the axis as compared to the density at the edges of the channel where the density is maximum. Therefore, the refractive index becomes maximum on the axis and decreases towards the edges. The use of an ignitor beam reduces the energy requirements for the heater beam and allows better control of plasma parameters and reproducibility shot-to-shot than a single beam configuration.

When the third laser beam is passed through the plasma channel, it tends to diffract due to diffraction and converge due to nonlinear refraction under the combined effects of density nonuniformity of the plasma channel and relativistic mass nonlinearity of plasma electrons (Akhiezer and Polovin, 1956). When both the convergence and divergence of the laser beam exactly balance each other, the laser beam propagates without any change in its spot size. However, in an axially nonuniform plasma channel, this condition cannot be satisfied throughout the plasma channel and hence the beam spot size changes as it propagates through the channel (Liu and Tripathi, 1994).

Laser–plasma interactions are perennially fraught with copious nonlinear effects such as electron plasma wave excitation (Purohit *et al.*, 2008, 2010), stimulated Raman scattering (Sharma *et al.*, 2013; Rawat *et al.*, 2014), stimulated Brillouin scattering (Sharma and Singh, 2013; Yadav *et al.*, 2016), higher harmonic generation (HHG) (Malka *et al.*, 1997; Gupta and Singh, 2016), and so on. Some of these phenomena lead to anomalous electron and ion heating and other to depleting or redirecting the incident laser flux and thus reduce the implosion efficiency of the fuel pellet in inertial confinement fusion. Therefore, to have deep insight into laser–plasma interaction physics, it becomes vital to investigate some of these phenomena by carrying out comprehensive studies encompassing theoretical as well as experimental aspects. Generation of higher harmonics of electromagnetic radiations in laser-produced plasmas is an important nonlinear process and has become an important field of research. Harmonic generation has a strong influence on the nature of laser propagation through plasmas. It allows penetration of laser power to over dense regions of the plasmas (Stamper *et al.*, 1985) and thus has become an important diagnostic tool for obtaining information about plasma parameters such as electrical conductivity, expansion velocity, opacity, local electron density, and so on, via interferometry or absorption spectroscopy (Teubner and Gibbon, 2009). A classic example of this is second harmonic generation (SHG), which is routinely used to track the passage of intense laser beams through underdense plasma targets. Ultrafast pulse duration and good spatial and temporal coherence of harmonic radiations make them a good candidate for applications in vacuum ultraviolet or extreme ultraviolet regions. This includes ultrafast ionization of atoms, molecules or clusters in strong fields of short wavelengths, ultrafast spatial interferometry, ultrafast holography to investigate dynamics of surface deformations.

Higher harmonic generation is not the only technique for the generation of coherent light at short wavelengths. For this, various techniques are available, such as synchrotrons and free electron lasers. However, due to the typical size and related costs, these facilities are rather exclusive and access to them is limited. This impedes the progress in the fields of research associated with these facilities. In contrast, light sources based on HHG are much less expensive and can be accommodated in a table top device. These advantaged can bring coherent short-wavelength radiation sources within the reach of less affluent institutions, such as universities and hospitals. Another disadvantage of

synchrotron radiations is that X-rays from synchrotrons cannot trace atomic motions inside a molecule or a solid. All we see is a dim blur, the pulses are nor short or bright enough. A synchrotron source can image molecules only if they are arranged in crystals, where the local forces hold millions of them in precise ranks like identical soldiers at attention. Laser harmonics, for their part, are brighter because they produce coherent light: The electromagnetic fields in laser harmonics are not choppy like the surface of a rough sea but smoothly oscillate with controlled regularity.

Harmonic generation of electromagnetic radiations in plasmas has been the subject of extensive study for quite some time. Early seminal works of Sodha *et al.* gave gravest blows to the studies on SHG of laser beams in plasmas (Sodha *et al.*, 1968, 1978). Hora and Ghatak (1985) derived and evaluated second harmonic resonance for perpendicular incidence at four times the critical density. Kant and Sharma (2004) investigated second harmonic generation of short laser pulse in plasma by taking into consideration the effect of pulse slippage. Sukhdeep *et al.* investigated resonant second harmonic generation of Gaussian laser beam in collisional magnetoplasma. Agarwal *et al.* (2001) studied the resonant second harmonic generation of a millimetre wave in plasma in the presence of magnetic wiggler. The wiggler provides an additional momentum for the generation of harmonic photon. Singh and Walia (2011a, 2011b, 2013) investigated the effect of self-focusing of Gaussian laser beam on second harmonic generation in collisional (2011a), collisionless (2011b), and relativistic (2013) plasmas by using moment theory approach. Jha and Aggarwal (2014) investigated the second harmonic generation of p-polarized laser beam in under dense plasma.

It is well-known fact that laser beams with different intensity profiles behave differently in plasmas. The investigations on SHG of laser beams in plasmas and plasma channels, till date, to the best of author's knowledge are limited to revealing the propagation characteristics of laser beams having Gaussian irradiance along their wavefronts. In contrast to this picture investigations on the intensity profile of the Vulcan Pettawatt laser at Rutherford Appelton laboratory by Patel *et al.* (2005) and Nakatsutsumi *et al.* (2008) suggest that the intensity profile of the laser beam is not exactly Gaussian but is having deviations from it. The suggested intensity profile that fits with the experimental data is q-Gaussian of the form $f(r) = f(0)(1 + (r^2/qr_0^2))^{-q}$, where the values of relevant parameters q and r_0 can be obtained by fitting the experimental data. The perturbations in the intensity profile of the laser beam may appear due to small obstacles of accidental nature (such as inclusions in the gain medium or in other optical elements of laser, dust particles etc). Fresnel diffraction on different apertures in a laser installation, including the hard edges of active elements, also play a prominent role in the origin of intensity perturbations. Literature review reveals the fact that no earlier theoretical investigation on SHG of q-Gaussian laser beams in plasma channels has been reported in the past. The aim of this paper is to investigate for the first time SHG of q-Gaussian Laser beam in plasma channel created by ignitor-heater technique.

Ionization of air

Consider the propagation of ignitor beam through air along z-axis. The field of the ignitor beam is given by

$$E_1(r, z, t) = E_1(r, z)e^{-\iota(\omega_0 t - k_0 z)}e_x$$

$$E_1 E_1^{\star} = \frac{E_{10}^2}{f_1^2} e^{-(r^2/r_0^2 f_1^2)} \qquad (1)$$

where $r_0 f_1$ is the instantaneous spot size of the ignitor beam. Hence, the parameter f_1 is known as dimensionless beam width parameter which is measure of both spot size and axial intensity of the ignitor beam. The beam ionizes the air via tunnel ionization. We take air that predominantly compris of nitrogen. Following Keldysh (1965), the rate of tunnel ionization of an atom is given by

$$\Gamma = \frac{4\pi e^4}{\hbar^3}\left(\frac{E_i}{E_a}\right)^{5/2}\left(\frac{E_a}{|E_1|}\right)e^{-(2/3)(E_a/|E_1|)(E_i/E_a)^{5/2}} \tag{2}$$

where E_i is the ionization potential of the atom, E_h is the ionization potential of hydrogen,

$$E_a = \frac{m^2 e^5}{\hbar^4} \simeq 1.7 \times 10^7 esu$$

is the atomic unit of electric field. The plasma density so formed is modeled by Liu and Tripathi (1994) as

$$\omega_p^2 = \omega_{p0}^2 e^{-(E'_a/|E_1|)} \tag{3}$$

where,

$$E'_a = \frac{2}{3}E_a\left(\frac{E_i}{E_h}\right)^{1/2}, \quad \omega_p^2 = \frac{4\pi e^2}{m_e}n_{e0} \quad \text{and} \quad \omega_{p0}^2 = \frac{4\pi e^2}{m_e}n_0.$$

The dielectric function of plasma is given by

$$\epsilon_1 = 1 - \frac{\omega_p^2}{\omega_0^2} \tag{4}$$

Using Eq. (3) in (4), we get

$$\epsilon_1 = 1 - \frac{\omega_{p0}^2}{\omega_0^2}e^{-(E'_a/|E_1|)} \tag{5}$$

Taking

$$\epsilon_1 = \epsilon_{01} + \phi_1(E_1 E_1^\star) \tag{6}$$

where $\epsilon_{01} = \epsilon_1|_{r=0}$ is the axial part of the dielectric function and ϕ_1 is the off-axial part of the dielectric function, we get

$$\epsilon_{01} = 1 - \frac{\omega_{p0}^2}{\omega_0^2}e^{-f_1(E'_a/E_{10})} \tag{7}$$

and

$$\phi_1(E_1 E_1^\star) = \frac{\omega_{p0}^2}{\omega_0^2}\left\{e^{-f_1(E'_a/E_{10})} - e^{-(f_1(E'_a/E_{10})e^{r^2/(2r_0^2 f_1^2)})}\right\} \tag{8}$$

Formation of plasma channel

In order to slow down the process of electron ion recombination and to prolong the plasma, one launches the second beam (heater beam)

$$E_2 = E_2(r, z)e^{-\iota(\omega_0 t - k_0 z)}e_x$$

$$E_2 E_2^\star = \frac{E_{20}^2}{f_2^2}e^{-(r^2/(r_0^2 f_2^2))} \tag{9}$$

It imparts oscillatory velocity to plasma electrons

$$v_2 = \frac{-eE_2(v_{ei} + \iota\omega_0)}{m_e\omega_0^2} \tag{10}$$

where v_{ei} is the electron-ion collision frequency. The electron temperature rises and heats them at an average rate $Re[-eE_2^\star.(v/2)]$. The energy balance equation for the electrons is (Kumar et al., 2010)

$$\frac{3}{2}\frac{dT_e}{dt} = \frac{e^2|E_2|^2 v_{ei}}{2m_e\omega_0^2} - \frac{3}{2}\delta v_{ei}[T_e - T_{e0}] \tag{11}$$

where δ is the mean fraction of excess energy lost per collision, T_e is the field-dependent electron temperature, and T_{e0} is the equilibrium plasma temperature. Taking the variation of electron-ion collision frequency with electron temperature as $v_{ei} = v_0(T_e/T_{e0})^{-(3/2)}$, v_0 is the electron-ion collision frequency at equilibrium plasma temperature. Equation (11) can be integrated to obtain the electron temperature as

$$T_e = T_{e0}\left[1 + \frac{\beta_2 E_{20}^2}{f_2^2}e^{-(r^2/r_0^2 f_2^2)}\right] \tag{12}$$

where $\beta_2 = (e^2 M/6K_0 T_{e0} m_e^2 \omega_0^2)$ is the coefficient of collisional nonlinearity. The nonuniformity in temperature leads to gradient in electron partial pressure and hence electrons move out from a high-temperature region to a low-temperature region. This creates a space charge field that pushes the ions along. A steady state is realized when the sum of the electron and ion partial pressures is uniform, $n_e T_e + n_i T_i = 2n_{e0} T_{e0}$. Taking $n_e \simeq n_i$, one obtains

$$n_e = \frac{2n_0 e^{-f_1(E'_a/E_1)}}{(1 + (T_e/T_{e0}))} \tag{13}$$

One may expand n_e in the powers of r as

$$n_e = n_1 + n_2\frac{r^2}{r_0^2}$$

where

$$n_1 = \frac{n_0 e^{-f_1(E'_a/E_{10})}}{1 + [1 + (\beta_2 E_{20}^2/f_2^2)]^{2/5}} \tag{14}$$

and

$$n_2 = \frac{2n_0 e^{-f_1(E'_a/E_{10})}(1 + (\beta_2 E_{20}^2/f_2^2))^{-3/5}\beta_2 E_{20}^2}{5\{1 + (1 + (\beta_2 E_{20}^2/f_2^2))^{2/5}\}^2 f_2^4} \tag{15}$$

The linear and nonlinear parts of the dielectric permittivity experienced by heater beam thus can be written as

$$\epsilon_{02} = 1 - \frac{\omega_{p0}^2}{\omega_0^2}\frac{e^{-f_1(E'_a/E_{10})}}{1 + (1 + (\beta_2 E_{20}^2/f_2^2))^{2/5}} \tag{16}$$

$$\phi_2 = -\frac{\omega_{p0}^2}{\omega_0^2}\frac{2}{5}\frac{\beta_2 E_{20}^2}{f_2^4}e^{-f_1(E_a'/E_{10})}\frac{(1+(\beta_2 E_{20}^2/f_2^2))^{-(3/5)}}{1+\{(1+(\beta_2 E_{20}^2/f_2^2))^{2/5}\}}\frac{r^2}{r_0^2} \quad (17)$$

Dielectric function of plasma channel for *q*-Gaussian laser beam

Consider the propagation of a circularly polarized *q*-Gaussian laser beam

$$E_3 = E_3(r,z)e^{-\iota(\omega_0 t - k_0 z)}(e_x + \iota e_y)$$

$$E_3 E_3^\star = \frac{E_{30}^2}{f_3^2}(1+(r^2/qr_0^2 f_3^2))^{-q} \quad (18)$$

through the plasma channel. Where the parameter *q* describes the deviation of the intensity profile of the laser beam from Gaussian distribution (Sharma and Kourakis, 2010; Wang *et al.*, 2017). Laser beams with lower values of *q* are characterized by expanded wings of the intensity distribution. As the value of *q* increases, the intensity profile of the laser beam converges towards Gaussian distribution and becomes exactly Gaussian for $q = \infty$ that is,

$$\lim_{q\to\infty} E_3 E_3^\star = \frac{E_{30}^2}{f_3^2}e^{-(r^2/r_0^2 f_3^2)}$$

The dielectric function of the plasma channel can be written as

$$\epsilon_3 = 1 - \frac{\omega_{p0}^2}{\omega_0^2}\frac{e^{-f_1(E_a'/E_{10})}}{1+(1+(\beta_2 E_{20}^2/f_2^2))^{2/5}}$$
$$-\frac{2}{5}\frac{\omega_{p0}^2}{\omega_0^2}\frac{\beta_2 E_{20}^2}{f_2^4}e^{-f_1(E_a'/E_{10})}\frac{(1+(/ta_2 E_{20}^2/f_2^2))^{-(3/5)}}{\{1+(1+(\beta_2 E_{20}^2/f_2^2))^{2/5}\}^2}\frac{r^2}{r_0^2} \quad (19)$$

The plasma electrons due to circularly polarized laser beam move along circular orbits with frequency ω_0. The quiver speed of electrons due to high field associated with the intense laser beam becomes comparable to that of light in vacuum. Hence, the effective mass m_e of electrons in Eq. (19) gets replaced by $m_0\gamma$, where m_0 is the rest mass of electron and γ is relativistic Lorentz factor. Following Akhiezer and Polovin at equilibrium

$$-eE_3 = \frac{m_0 v\omega_0}{(1-(v^2/c^2))^{1/2}} \quad (20)$$

where *c* is the speed of light in vacuum and *v* is the quiver velocity of electron in the field of the laser beam. From Eqs (18) and (20) we get

$$\gamma = \left\{1+\frac{\beta_3 E_{30}^2}{f_e^2}(1+(r^2/qr_0^2 f_3^2))^{-q}\right\}^{1/2} \quad (21)$$

Hence, the effective dielectric function of the plasma channel for *q*-Gaussian laser beam can be written as

$$\epsilon_{03} = 1 - \frac{\omega_{p0}'^2}{\omega_0^2}\frac{e^{-f_1(E_a'/E10)}}{\{1+(1+(\beta_2 E_{20}^2/f_2^2))^{2/5}\}}(1+(\beta_3 E_{30}^2/f_3^2))^{-1/2} \quad (22)$$

$$\phi_3 = \frac{\omega_{p0}'^2}{\omega_0^2}\frac{e^{-f_1(E_a'/E_{10})}}{\{1+(1+(\beta_2 E_{20}^2/f_2^2))^{2/5}\}}\left(1+\frac{\beta_3 E_{30}^2}{f_3^2}\right)^{-1/2}$$
$$\left\{\frac{\omega_{p0}'^2}{\omega_0^2}\frac{e^{-f_1(E_a'/E_{10})}}{\{1+(1+(\beta_2 E_{20}^2/f_2^2))^{2/5}\}^2}\frac{r^2}{r_0^2}\right\}\left(1+\frac{\beta_3 E_{30}^2}{f_3^2}\left(1+\frac{r^2}{qr_0^2 f_3^2}\right)\right)^{-1/2} \quad (23)$$

where

$$\omega_{p0}'^2 = \frac{4\pi e^2}{m_0}n_0$$

Spot size evolution of the laser beams

Starting from Ampere's and Faraday's laws for ab isotropic, non-conducting and non absorbing medium ($J = 0$, $\rho = 0$, $\mu = 1$), we get

$$\nabla \times B_j = \frac{1}{c}\epsilon_j\frac{\partial E_j}{\partial t} \quad (24)$$

$$\nabla \times E_j = -\frac{1}{c}\frac{\partial B_j}{\partial t} \quad (25)$$

where $j = 1 - 3$. Combining Eqs (24) and (25), it can be shown that the electric field vectors $E(r, z, t)$ of the laser beams satisfy the wave eqn

$$\nabla^2 E_j - \nabla(\nabla.E_j) + \frac{\omega_0^2}{c^2}\epsilon_j E_j = 0 \quad (26)$$

Even if E_j has longitudinal components, the polarization term $\nabla(\nabla.E_j)$ of Eq. (26) can be neglected, provided

$$\frac{c^2}{\omega_0^2}\left|\frac{1}{\epsilon_j}\nabla^2\ln\epsilon_j\right| \ll 1$$

that is, the transverse gradient of the dielectric function is small as compared to the laser wavelength. This implies that either the transverse dielectric variations are weak or the plasma is significantly underdense under this approximation Eq. (26) reduces to

$$\nabla^2 E_j + \frac{\omega_0^2}{c^2}\epsilon_j E_j = 0 \quad (27)$$

using Eqs (1), (9) and (18) in (27) we get

$$\iota\frac{\partial E_j}{\partial z} = \frac{1}{2k_0}\nabla_\perp^2 E_j + \frac{k_0}{2\epsilon_{0j}}\phi_j(E_j E_j^\star)E_j \quad (28)$$

In deriving Eq. (28), the term $(d^2 E_j/dz^2)$ has been neglected under the assumption $|(d^2 E_j/dz^2)| \ll k_0^2 E_j$ that implies much longer wave amplitude scale length along the longitudinal direction as compared to the wavelength.

Now, definition of second order spatial moment (Lam *et al.*, 1975, 1977) of intensity distribution, the mean square radius of a laser beam is given by

$$\langle a_j^2\rangle = \frac{1}{I_{0j}}\int_0^{2\pi}\int_0^\infty r^2 E_j E_j^\star r\,dr\,d\theta \quad (29)$$

where

$$I_{0j} = \int_0^{2\pi} \int_0^{\infty} E_j E_j^{\star} \, r dr d\theta \tag{30}$$

Diffrentiating Eq. (29) twice with respect to z and substituting the values of dE_j/dz and $dE_z^{\star}/dz$ from Eq. (28), we get

$$I_{0j} \frac{d^2}{dz^2} \langle a_j^2 \rangle = \frac{2}{k_0^2} \left[\frac{1}{k_0} \int_0^{2\pi} \int_0^{\infty} |\nabla_{\perp} E_j|^2 r dr d\theta \right.$$
$$\left. + \frac{k_0}{2\varepsilon_{0j}} \int_0^{2\pi} \int_0^{\infty} r^2 E_j E_j^{\star} \frac{\partial \phi_j}{\partial r} dr d\theta \right] \tag{31}$$

Using Eqs (1), (7)–(9), (16)–(18), (22), (23), (29), (30) in (31) we get following set of coupled differential eqs governing the evolution of spot size of the laser beams with distance of propagation

$$\frac{d^2 f_1}{d\eta^2} + \frac{1}{f_1} \left(\frac{df_1}{d\xi} \right)^2 = \frac{1}{f_1^3} + 2 \frac{E_a'}{E_{10}} \left(\frac{\omega_{p0}^2 r_0^2}{c^2} \right) I_1 \tag{32}$$

$$\frac{d^2 f_2}{d\eta^2} + \frac{1}{f_2} \left(\frac{df_2}{d\xi} \right)^2$$
$$= \frac{1}{f_2^3} - \frac{2}{5} \left(\frac{\omega_{p0}^2 r_0^2}{c^2} \right) \frac{\beta_2 E_{20}^2}{f_2^2} e^{-f_1(E_a'/E_{10})} \frac{(1 + (\beta_2 E_{20}^2/f_2^2))^{-3/5}}{(1 + (1 + (\beta_2 E_{20}^2/f_2^2))^{2/5})^2} \tag{33}$$

$$\frac{d^2 f_3}{d\eta^2} + \frac{1}{f_3} \left(\frac{df_3}{d\xi} \right)^2 = \left(1 - \frac{1}{q} \right) \left(1 - \frac{2}{q} \right)$$
$$\times \left[\frac{1}{(1 + (1/q)) f_3^3} - \frac{1}{2} \frac{\beta_2 E_{20}^2}{f_3^3} \left(\frac{\omega_{p0}^2 r_0^2}{c^2} \right) \right]$$

$$\frac{e^{-f_1(E_a'/E_10)}}{(1 + (1 + (\bar{e}ta_2 E_{20}^2/f_2))^{2/5})} K_1$$
$$- \frac{1}{5} \left(\frac{\omega_{p0^2} r_0^2}{c^2} \right) \frac{\beta_2 E_{20}^2}{f_2^4} e^{-f_1(E_a'/E_{10})} \frac{(1 + (\beta_2 E_{20}^2/f_2^2))^{-3/5}}{(1 + (1 + (\beta_2 E_{20}^2/f_2^2))^{2/5})^2}$$
$$\times \left(2 f_3 K_2 + \frac{\beta_3 E_{30}^2}{f_3} K_3 \right) \tag{34}$$

where

$$I_1 = \int_0^{\infty} x e^{-x} e^{-(f_1(E_a'/E_{10}) e^x)} dx$$

$$K_1 = \int_0^{\infty} y \left(1 + \frac{y}{q} \right)^{-2q-1} \left\{ 1 + \frac{\beta_3 E_{30}^2}{f_3^2} \left(1 + \frac{y}{q} \right)^{-q} \right\}^{-(3/2)}$$

$$K_2 = \int_0^{\infty} y \left(1 + \frac{y}{q} \right)^{-q} \left\{ 1 + \frac{\beta_3 E_{30}^2}{f_3^2} \left(1 + \frac{y}{q} \right)^{-q} \right\}^{-(1/2)}$$

$$K_3 = \int_0^{\infty} y \left(1 + \frac{y}{q} \right)^{-2q-1} \left\{ 1 + \frac{\beta_3 E_{30}^2}{f_3^2} \left(1 + \frac{y}{q} \right)^{-q} \right\}^{-(1/2)}$$

$$x = \frac{r^2}{r_0^2 f_1^2}$$

$$y = \frac{r^2}{r_0^2 f_3^2}$$

$$\xi = \frac{z}{k_0 r_0^2}$$

For initially plane wavefronts Eqs (32)–(34) are subjected to boundary conditions $f_j = 1$, $\frac{df_j}{d\xi} = 0$ at $\xi = 0$.

Excitation of electron plasma wave

Electron plasma wave (EPW) can be generated by intense laser beams propagating through plasmas, due to medium's remarkable properties. Plasma as a whole is electrically neutral, containing equal amounts of negative (electrons) and positive charge (ions). An intense laser beam propagating through plasma creates a disturbance in the plasma. In essence, the beam pushes the lighter particles (electrons) away from the heavier positive ions, which in turn get left behind, creating a region of excess positive charge and a region of excess negative charge. Such an uneven distribution of charge sets up an electric field, which runs from positive to negative regions. The electric field pulls the electrons and ions together with equal force. Since the electron's mass is much smaller than that of ions, the electrons move towards the positive regions, whereas the ions remain essentially at rest. As the electrons from negative regions are drawn to the positive regions, they steadily gain velocity and momentum. The momentum does more than carry the electrons to a positive region: It causes them to overshoot it, whereupon the electric field reverses its direction, first opposing the electron's motion and slowing them down and then pulling them back again. The process repeats itself and forms a longitudinal wave of positive and negative regions traveling through the plasma. The generated plasma wave is governed by equation of continuity, equation of motion, equation of state and Poisson's equation.

$$\frac{\partial N_e}{\partial t} + \nabla(N_e v) = 0 \tag{35}$$

$$\frac{\partial(N_e v)}{\partial t} + \nabla(N_e v^2) + \frac{1}{m_e} \nabla P_e + \frac{N_e e E_0}{m_e} = 0 \tag{36}$$

$$\frac{P_e}{N_e^{\gamma}} = constant \tag{37}$$

$$\nabla E_0 = 4\pi(ZN_{0i} - N_e)e \tag{38}$$

Using linear perturbation theory, Eqs (35)–(38) give the equation for plasma wave as follows

$$-\omega_0^2 n + v_{th}^2 \nabla^2 n + \omega_p^2 n = \frac{e}{m} n_0 \nabla E_3 \tag{39}$$

For q-Gaussian laser beam solution of this wave equation gives the higher harmonic source term

$$n = \frac{en_0}{m} \frac{E_{30}}{r_0^2 f_3^3} \frac{r}{(\omega_0^2 - k_0^2 v_{th}^2 - \omega_p^2(N_{0e}/N_0))} \left(1 + \frac{r^2}{qr_0^2 f_3^2}\right)^{(-(q/2)-1)} \tag{40}$$

Second harmonic generation

The wave equation governing the electric field E_2' of second harmonic is given by

$$\nabla^2 E_2' + \frac{\omega_2^2}{c^2} \epsilon_2'(\omega_2) E_2' = \frac{\omega_p^2}{c^2} \frac{n}{n_0} E_3 \tag{41}$$

where $\omega_2 = 2\omega_0$ is frequency of second harmonic and ϵ_2' is the effective dielectric constant at second harmonic frequency. From the above equation the expression for field E_2' of second harmonic is obtained as

$$E_2' = \frac{\omega_p^2}{c^2} \frac{n}{n_0} \frac{E_0}{(k_2^2 - 4k_0^2)} \tag{42}$$

Now the second harmonic power can be written as

$$P_2 = \int_0^{2\pi} \int_0^\infty E_2 E_2^\star r dr d\theta \tag{43}$$

also, the power of initial pump beam is given by

$$P_0 = \int_0^{2\pi} \int_0^\infty E_0 E_0^\star r dr d\theta \tag{44}$$

Defining conversion efficiency of second harmonics as

$$Y_2 = \frac{P_2}{P_0} = \frac{K_0 T_0}{mc^2} \frac{c^2}{r_0^2 \omega_{p0}'^2} \frac{\omega_0^2}{\omega_{p0}'^2} \frac{\beta E_{30}^2}{f_3^4} \left(1 - \frac{1}{q}\right) H \tag{45}$$

where

$$H = \int^y \left(1 + \frac{y}{q}\right)^{-2q-2}$$
$$\times \frac{(\alpha_1 + \alpha_2 f_3^2 y)^2}{\{(\omega_0^2/\omega_{p0}'^2)\alpha_1 - \alpha_1 \epsilon_{03}(v_{th}^2/c^2)(\omega_0^2/\omega_{p0}'^2)}$$
$$-(\alpha_1 + f_3^2 y \alpha_2)(1 + (\beta_3 E_{30}^2/f_3^2)(1 + cyq)^{-q})^{-(3/2)}\}^2 \tag{46}$$

$$\alpha_1 = \left(\frac{\omega_{p0}'^2 r_0^2}{c^2}\right) \frac{e^{-f_1(E_a'/E_{10})}}{\{1 + (1 + (\beta_2 E_{20}^2/f_2^2))^{2/5}\}}$$

$$\alpha_2 = \left(\frac{\omega_{p0}'^2 r_0^2}{c^2}\right) \frac{\beta_2 E_{20}^2}{f_2^4} e^{-f_1(E_a'/E_{10})} \frac{(1 + (\beta_2 E_{20}^2/f_2^2))^{-(3/5)}}{\{1 + (1 + (\beta_2 E_{20}^2/f_2^2))^{2/5}\}^2}$$

Discussion

Equations (32)–(34) describe the evolution of dimensionless beam width parameters f_j of the laser beams and Eq. (45) describes the conversion efficiency of the second harmonics with distance of propagation. There are two terms on the right-hand side (RHS) of Eqs (32)–(34), each representing some physical mechanism responsible for the evolution of beam envelope during its propagation. The first term that has its origin in the Laplacian ($\nabla_\perp^2$) in wave Eq. (28) is responsible for the diffraction broadening of the laser beam and is therefore termed as diffractive term. The second term arises due to laser induced nonlinearity in the dielectric properties of the medium and is responsible for the nonlinear refraction of the laser beam. Depending on the relative competition between these two terms one can observe focusing/defocusing of the laser beam. Equations (32)–(34) and (45) have been solved numerically for following set of parameters:

$$\omega_0 = 1.78 \times 10^{15} \text{ rad/sec}$$

$$r_0 = 15 \,\mu\text{m}$$

$$n_0 = 10^{17} \text{ cm}^{-3}$$

$$T_{e0} = 10^6 \text{K}$$

Figures 1, 2, 3 illustrate the effect of the intensity of first beam (ignitor beam) on the evolution of the spot size of the laser beams with distance of propagation. The plots in Figure 1 depict that as the ignitor beam propagates through the air its spot size increases monotonically. This is due to the fact that nonlinear refraction of the ignitor beam favors the natural diffraction due to ionization induced defocusing. It is also observed that with increase in the intensity of ignitor beam the rate of its defocusing decreases. This is due to the fact that increase in the intensity of ignitor beam leads to decrease in its nonlinear refraction.

The plots in Figure 2 depict that as second beam (heater beam) propagates through the plasma, initially its spot size shows oscillatory focusing and then its spot size starts increasing monotonically. This is due to the fact that the plasma is being created by the ignitor beam. Initially, it is intense enough to create sufficient ionization of the air so that the plasma density is enough for the self-focusing of the heater beam. But as the ignitor beam gets defocused with distance of propagation, its intensity goes on decreasing and hence the plasma density becomes less than that required for the self-focusing of the heater beam.

It is also observed that with increase in the intensity of ignitor beam, the rate of defocusing of the heater beam decreases. This is due to the fact that with increase in the intensity of ignitor beam, the magnitude of refractive term opposing the diffractive term in
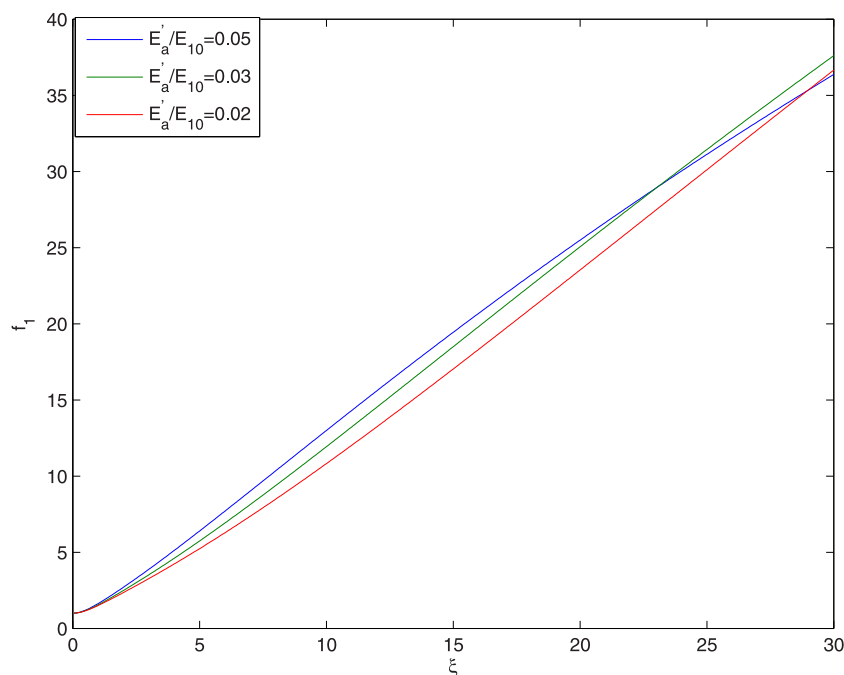
Fig. 1. Evolution of spot size of ignitor beam with distance of propagation at different intensities of ignitor beam viz. $E'_a/E_{10} = 0.05, 0.03, 0.02$ and at fixed values of $\beta_2 E_{20}^2 = 2.5$, $\beta_3 E_{30}^2 = 3$ and $q = 3$.
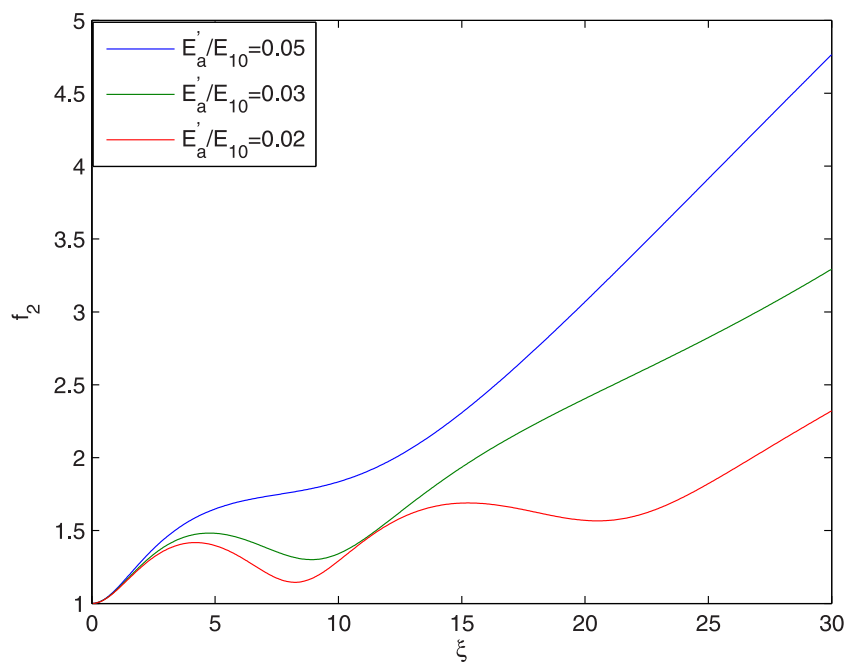

Fig. 2. Evolution of spot size of heater beam with distance of propagation at different intensities of ignitor beam viz. $E'_a/E_{10} = 0.05, 0.03, 0.02$ and at fixed values of $\beta_2 E_{20}^2 = 2.5$, $\beta_3 E_{30}^2 = 3$ and $q = 3$.

Eq. (33) increases that leads to decrease in the rate of defocusing of the heater beam.

The plots in Figure 3 depict that as the third laser beam propagates through the plasma channel its beam width oscillates periodically, but after every focal spot the maxima and minima of the spot size shifts upwards. This is due to the fact that as the intense q-Gaussian laser beam is shone into the plasma channel, due to the large amplitude of the electric filed associated with the laser beam, the quiver velocity of the plasma electrons becomes comparable to that of light in vacuum. As a result of this, the mass of plasma electrons increases and hence the plasma frequency

reduces. At the beam center, where the intensity is maximum, the mass of electrons is maximum and hence the plasma frequency is minimum. As a result of this, the central part of the wavefront of the laser beam experiences maximum refractive index due to which the wavefronts of the laser beam bend inwards resulting in self-focusing of the laser beam. As the laser beam gets self-focused with distance of propagation, its spot size $r_0 f_3$ decreases which leads to increase in diffraction opposing the non-linear refraction. This slows down focusing till minimum of f_3 is obtained. The diffraction effects then become dominant but not sufficient to overcome self-focusing. The process goes on till
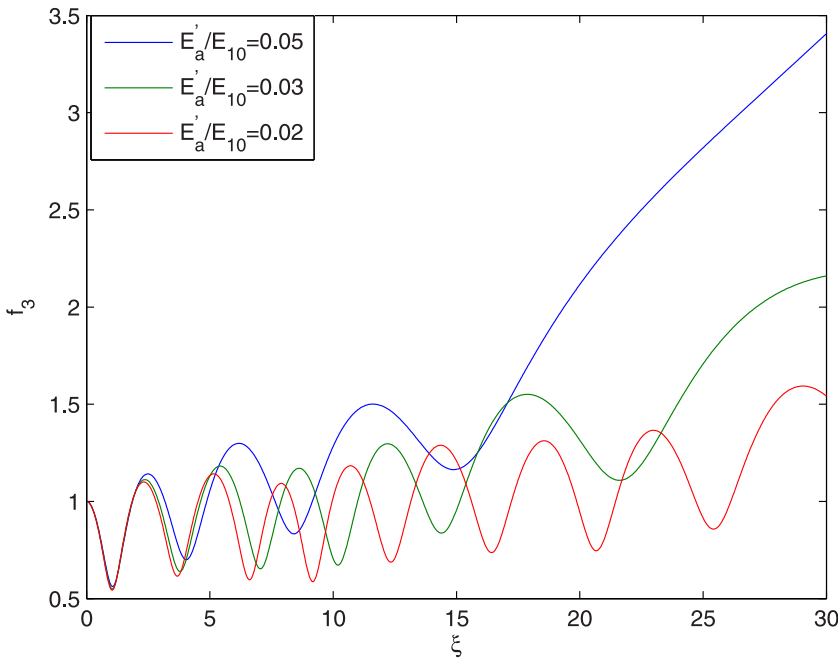
Fig. 3. Evolution of spot size of guided beam with distance of propagation at different intensities of ignitor beam viz. $E'_a/E_{10} = 0.05, 0.03, 0.02$ and at fixed values of $\beta_2 E_{20}^2 = 2.5$, $\beta_3 E_{30}^2 = 3$ and **q** = 3.
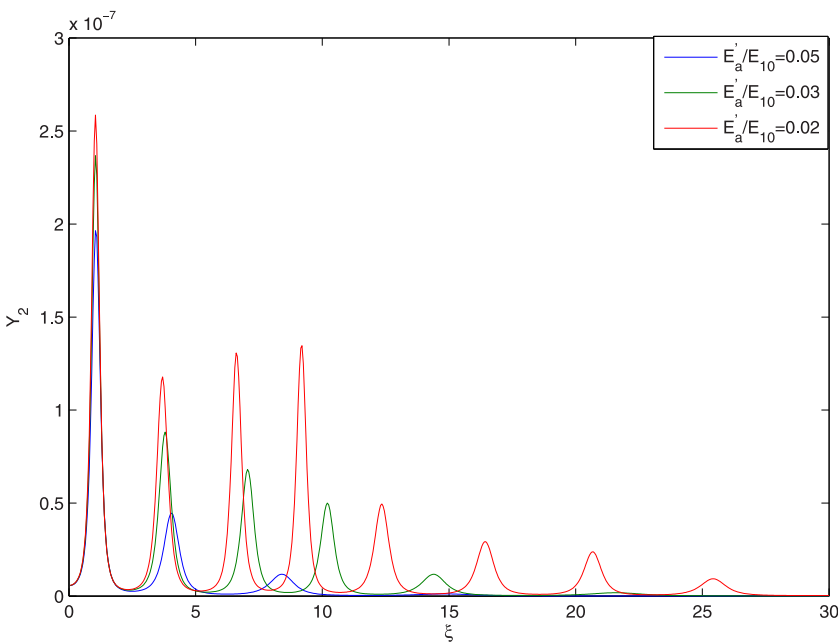

Fig. 4. Evolution of harmonic yield Y_2 of guided beam with distance of propagation at different intensities of ignitor beam viz. $E'_a/E_{10} = 0.05, 0.03, 0.02$ and at fixed values of $\beta_2 E_{20}^2 = 2.5$, $\beta_3 E_{30}^2 = 3$ and **q** = 3.

diffraction effect overpower the nonlinear refraction of the laser beam. These processes go on repeating themselves leading to oscillatory focusing/defocusing of the laser beam. The spot size of the laser beam thus oscillates or scallop periodically in sausage like fashion as the laser beam propagates down the channel.

Upward shifting of the minima of f_3 with distance of propagation is due to the decreasing plasma density resulting from the diffraction of the ignitor beam.

It is also observed that with increase in the intensity of the ignitor beam there is a significant increase in the effective distance of propagation of the third laser beam through the plasma channel. The underlying physics behind this fact is that with increase in the intensity of the ignitor beam there is decrease in the

diffraction of heater beam that creates the channel. This leads to enhanced radial inhomogeneity in the refractive properties of the plasma channel resulting in enhanced propagation of the third beam through the plasma channel.

Figure 4 illustrates the effect of the intensity of ignitor beam on evolution of conversion efficiency Y_2 of second harmonics with distance of propagation. It has been observed that the conversion efficiency of the second harmonics is maximum at the focal spots of the guided beam. This is due to the fact that the focal spots of the laser beam are the regions of maximum intensity. Hence the amplitude of the generated plasma wave is maximum there resulting in maximum conversion efficiency of the second harmonics. It is also observed that increase in the intensity of the ignitor
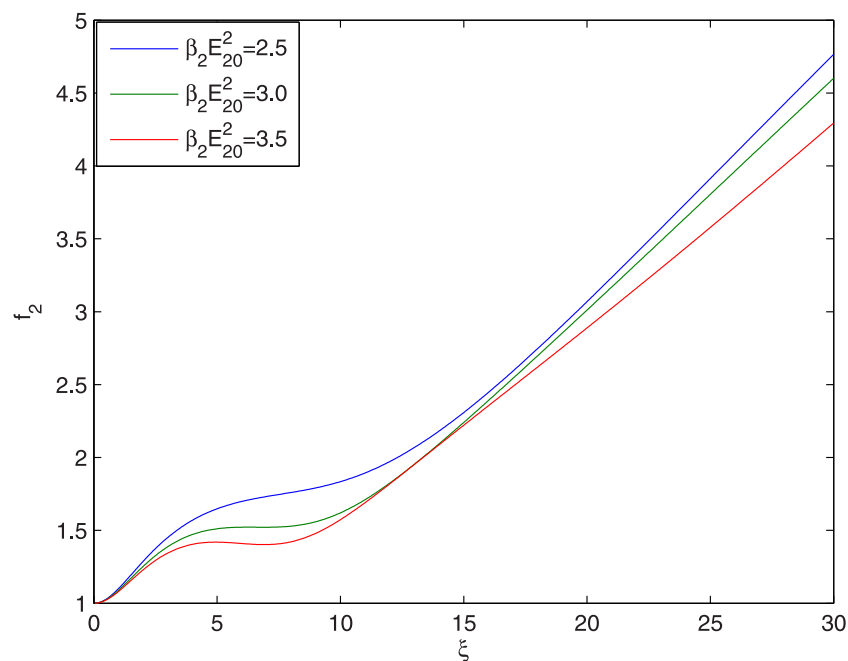
Fig. 5. Evolution of spot size of heater beam with distance of propagation at different intensities of heater beam viz. $\beta_2 E_{20}^2 = 2.5, 3, 3.5$ and at fixed values of $E'_a/E_{10} = 0.05$, $\beta_3 E_{30}^2 = 3$ and $\boldsymbol{q} = 3$.
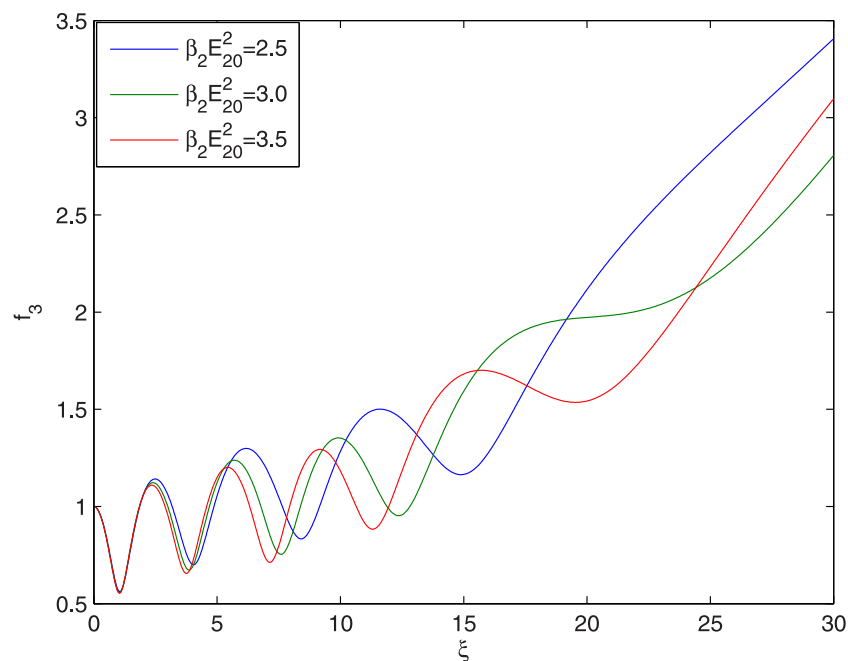

Fig. 6. Evolution of spot size of guided beam with distance of propagation at different intensities of heater beam viz. $\beta_2 E_{20}^2 = 2.5, 3, 3.5$ and at fixed values of $E'_a/E_{10} = 0.05$, $\beta_3 E_{30}^2 = 3$ and $\boldsymbol{q} = 3$.

beam leads to increase in the conversion efficiency of the second harmonics. This is due to the fact that there is one to one correspondence between the extent of the self-focusing of guided beam and conversion efficiency of its second harmonics. As there is increase in the extent of self-focusing of guided beam with increase in the intensity of ignitor beam, there is increase in conversion efficiency of second harmonics with increase in the intensity of ignitor beam.

Figures 5 and 6 illustrate the effect of intensity of the heater beam on evolution of the spot size of second and third laser beam with distance of propagation. The plots in Figure 5 depict that with increase in the intensity of heater beam there is decrease

in the rate of its defocusing. This is due to the fact that increase in the intensity of heater beam leads to enhanced heating of the plasma resulting in decrease in the rate of defocusing of the heater beam.

The plots in Figure 6 depict that increase in the intensity of heater beam enhances the effective distance of propagation of third beam through the plasma channel. This is due to the enhancement of the radial inhomogeneity in the refractive properties of the plasma channel with increase in the intensity of the heater beam.

The plots in Figure 7 illustrate the effect of intensity of heater beam on the evolution of conversion efficiency of second
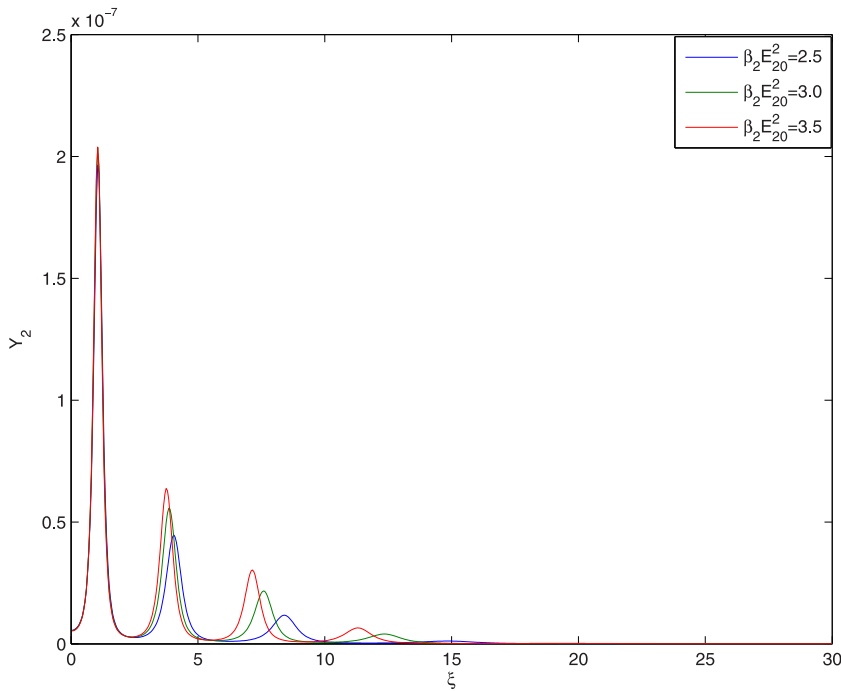
Fig. 7. Evolution of second harmonic yield Y_2 of guided beam with distance of propagation at different intensities of heater beam viz. $\beta_2 E_{20}^2 = 2.5, 3, 3.5$ and at fixed values of $E'_a/E_{10} = 0.05$, $\beta_3 E_{30}^2 = 3$ and **q** = 3.
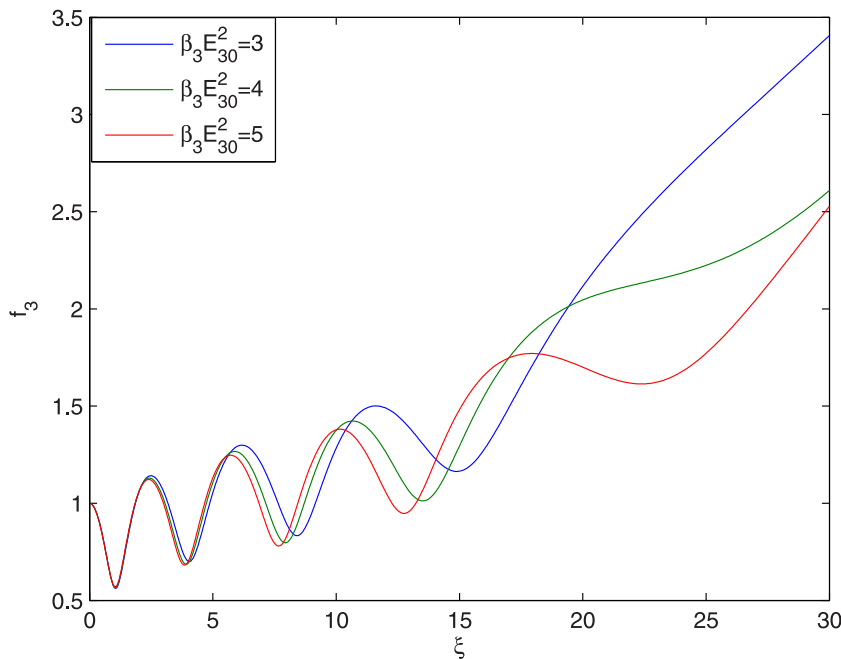

Fig. 8. Evolution of spot size of guided beam with distance of propagation at different intensities viz. $\beta_3 E_{30}^2 = 3, 4, 5$ and at fixed values of $E'_a/E_{10} = 0.05$, $\beta_2 E_{20}^2 = 2.5$ and **q** = 3.

harmonics of the guided beam. It has been observed that with increase in the intensity of heater beam there is increase in the conversion efficiency of second harmonics of guided beam. This is due to the fact that with increase in the intensity of heater beam there is increase in the extent of self-focusing of guided beam.

Figure 8 illustrates the effect of intensity of the third beam on evolution of its spot size with distance of propagation. It is observed that increase in the intensity of the third beam leads to increase in its effective distance of propagation through the plasma channel. It is due to increase in the relativistic nonlinearity in the electron mass with increase in intensity of third beam.

The plots in Figure 9 illustrate the effect of intensity of third beam on the evolution of conversion efficiency of its second harmonics. It has been observed that with increase in the intensity of third beam there is increase in the conversion efficiency ofits second harmonics. This is due to the fact that with increase in the intensity of third beam there is increase in the extent of its self-focusing.

Figure 10 illustrates the effect of deviation of intensity profile (i.e., the effect of q) of the third beam from Gaussian profile, on the evolution of its spot size with distance of propagation. It is observed that with increase in the value of q there is decrease in the effective distance of propagation of third beam through
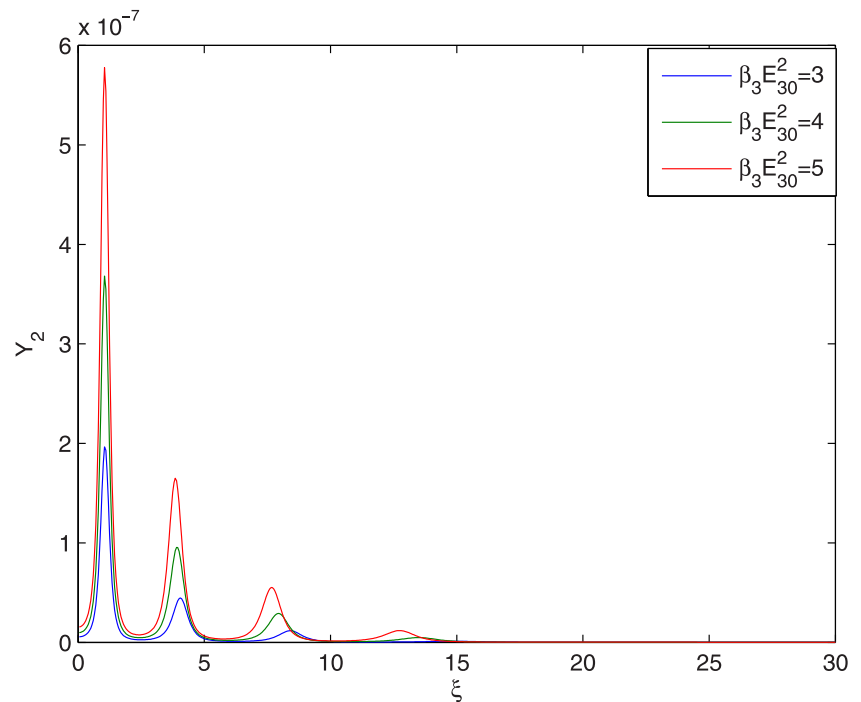
Fig. 9. Evolution of second harmonic yield Y_2 of guided beam with distance of propagation at different intensities viz. $\beta_3 E_{30}^2 = 3, 4, 5$ and at fixed values of $E_a'/E_{10} = 0.05$, $a_2 E_{20}^2 = 2.5$ and $\textbf{\textit{q}} = 3$.
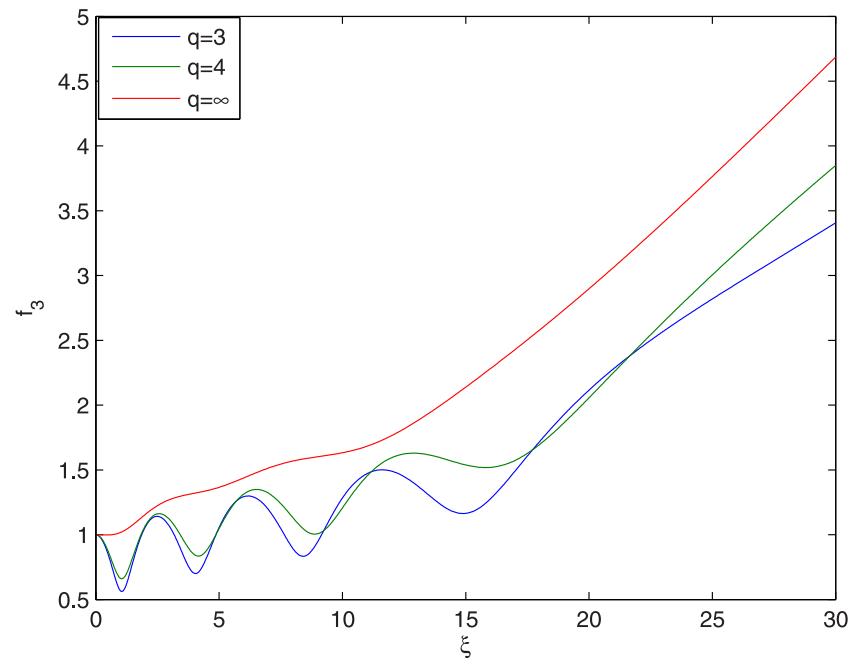

Fig. 10. Evolution of spot size of guided beam with distance of propagation at different values of $\textbf{\textit{q}}$ viz. $\textbf{\textit{q}} = 3, 4, \infty$ and at fixed values of $E_{10}/E_a' = 0.05$, $\beta_2 E_{20}^2 = 2.5$ and $\beta_3 E_{30}^2 = 3$.

the plasma channel. This is due to the fact that with increase in the value of q, the intensity of the laser beam converges towards the axial region of the wavefront. Hence, laser beams with higher values of q possess smaller root mean square radius. Also, it is well-known fact that the diffraction divergence of the laser beam is inversely proportional to its beam width. Hence, with increase in the value of q, the magnitude ofdiffractive term in Eq. (34) increases. Also, with increase in the value of q, the magnitude of nonlinear refractive term decreases due to the weakening of the axial part of the wavefront of the laser beam. As a result of this, the increase in the value of q leads to decrease in the effective distance of propagation of the third laser beam through the plasma channel.

Figure 11 depicts the effect of q value of guided beam on conversion efficiency of its second harmonics. It has been observed that with increase in the value of q there is decrease in the conversion
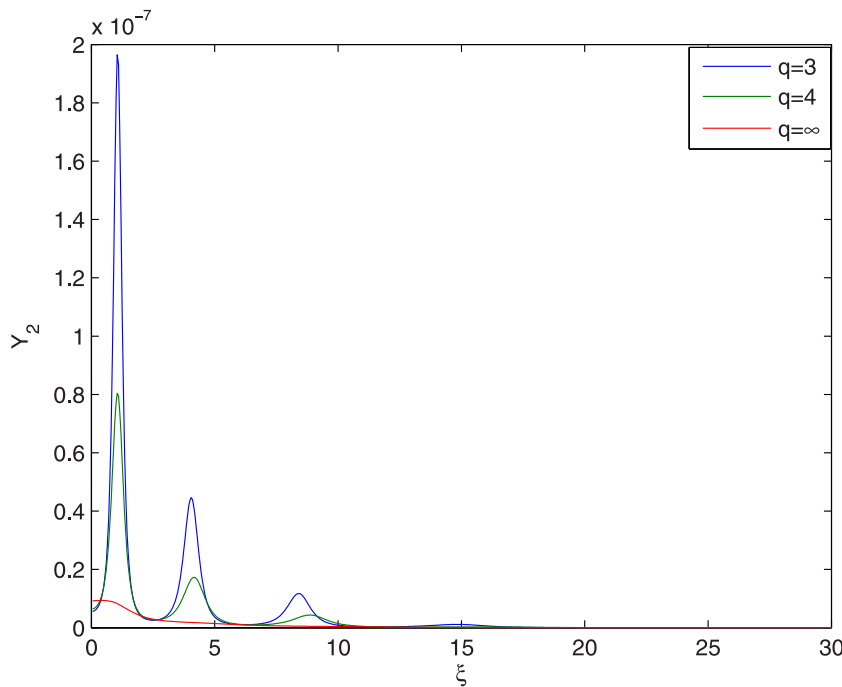
Fig. 11. Evolution of second harmonic yield Y_2 of guided beam with distance of propagation at different values of q viz. $q = 3$, 4, ∞ and at fixed values of $E_{10}/E_a' = 0.05$, $\beta_2 E_{20}^2 = 2.5$ and $\beta_3 E_{30}^2 = 3$.

efficiency of the second harmonics. This is due to the reduced focusing of the guided beam with increase in the value of q.

References

Agarwal RN, Pandey BK and Sharma AK (2001) Resonant second harmonic generation of a millimeter wave in a plasma filled waveguide. *Physica Scripta* **63**, 243.

Akhiezer AI and Polovin RV (1956) Theory of Wave Motion of an Electron Plasma. *Soviet Physics JETP* **3**, 696.

Clark TR and Milchberg HM (1997) Time and space-resolved density evolution of the plasma waveguide. *Physical Review Letters* **78**, 2373.

Clayton CE, Tzeng KC, Gordon D, Muggli P, Mori WB, Joshi C, Malka V, Najmudin Z, Modena A, Neely D and Dangor AE (1998) Plasma wave generation in a self-focused channel of a relativistically intense laser pulse. *Physical Review Letters* **81**, 100.

Ehrlich Y, Cohen C, Zigler A, Krall J, Sprangle P and Esarey E (1996) Guiding of high intensity laser pulses in straight and curved plasma channel experiments. *Physical Review Letters* **77**, 4186.

Esarey E, Sprangle P, Krall J and Ting A (1997) Self-focusing and guiding of short laser pulses in ionizing gases and plasmas. *IEEE Journal of Quantum Electronics* **33**, 1879.

Esarey E, Schroeder CB and Leemans WP (2009) Physics of laser-driven plasma-based electron accelerators. *Reviews of Modern Physics* **81**, 1229.

Faenov AY, Magunov AI, Pikuz TA, Skobelev IY, Gasilov SV, Stagira S, Calegari F, Nisoli M, Silvestri S, Poletto L, Villoresi P and Andreev AA (2007) X-ray spectroscopy observation of fast ions generation in plasma produced by short low-contrast laser pulse irradiation of solid targets. *Laser and Particle Beams* **25**, 267.

Gupta N and Singh A (2016) Second harmonic generation of self-focused cosh-Gaussian laser beam in thermal quantum plasma by excitation of an electron plasma wave. *Contributions to Plasma Physics* **56**, 889.

Hora H and Ghatak AK (1985) New electrostatic resonance driven by laser radiation at perpendicular incidence in superdense plasmas. *Physical Review A* **31**, 3473.

Jha P and Aggarwal E (2014) Second harmonic generation by propagation of a p-polarized obliquely incident laser beam in underdense plasma. *Physics of Plasmas* **21**, 053107.

Johnson JL, Dorney TD and Mittleman DM (2001) Enhanced depth resolution in terahertz imaging using phase-shift interferometry. *Applied Physics Letters* **78**, 835.

Kant N and Sharma AK (2004) Effect of pulse slippage on resonant second harmonic generation of a short pulse laser in a plasma. *Journal of Physics D: Applied Physics* **37**, 998.

Keldysh LV (1965) Ionization in the field of a strong electromagnetic wave. *Soviet Physics JETP* **20**, 1307.

Kumar A, Dahiya D and Sharma AK (2010) Laser prepulse induced plasma channel formation in air and relativistic self focusing of an intense short pulse. *Physics of Plasmas* **18**, 023102.

Lam JF, Lippmann B and Tappert F (1975) Moment theory of self-trapped laser beams with nonlinear saturation. *Optics Communications* **15**, 419.

Lam JF, Lippmann B and Tappert F (1977) Self-trapped laser beams in plasma. *Physics of Fluids* **20**, 1176.

Leemans WP, Clayton CE, Mori WB, Marsh KA, Kaw PK, Dyson A, Joshi C and Wallace JM (1992) Experiments and simulations of tunnel-ionized plasmas. *Physical Review A* **46**, 1091.

Liu CS and Tripathi VK (1994) Laser guiding in an axially nonuniform plasma channel. *Physics of Plasmas* **1**, 3100.

Malka V, Modena A, Najmudin Z, Dangor AE, Clayton CE, Marsh KA, Joshi C, Danson C, Neely D and Walsh FN (1997) Second harmonic generation and its interaction with relativistic plasma waves driven by forward Raman instability in underdense plasmas. *Physics of Plasmas* **4**, 1127.

Modena A, Najmudin Z, Dangor AE, Clayton CE, Marsh KA, Joshi C, Malka V, Darrow CB, Danson C, Neely D and Walsh FN (2002) Electron acceleration from the breaking of relativistic plasma waves. *Nature* **377**, 606.

Nakatsutsumi M, Davies JR, Kodama R, Green JS, Lancaster KL, Akli KU, Beg FN, Chen SN, Clark D, Freeman RR, Gregory CD, Habara H, Heathcote R, Hey DS, Highbarger K, Jaanimagi P, Key MH, Krushelnick K, Ma T, MacPhee A, MacKinnon AJ, Nakamura H, Stephens RB, Storm MM, Tampo, Theobald W, Woerkom LV, Weber RL, Wei MS, Woolsey NC and Norreys PA (2008) Space and time resolved measurements of the heating of solids to ten million kelvin by a petawatt laser. *New Journal of Physics* **10**, 043046.

Patel PK, Key MH, Mackinnon AJ, Berry R, Borghesi M, Chambers DM, Chen H, Clarke, Damian C, Eagleton R, Freeman R, Glenzer S, Gregori G, Heathcote R, Hey D, Izumi N, Kar S, King J, Nikroo A, Niles A, Park HS, Pasley J, Patel N, Shepherd R, Snavely RA, Steinman D, Stoeckl C, Storm M, Theobald W, Town R, Maren RV, Wilks SC and Zhang B (2005) Integrated laser–target interaction experiments on the RAL petawatt laser. *Plasma Physics and Controlled Fusion* **47**, B833.

Purohit G, Chauhan PK and Sharma RP (2008) Dynamics of the excitation of an upper hybrid wave by a rippled laser beam in magnetoplasma. *Physics of Plasmas* **15**, 052101.

Purohit G, Sharma P and Sharma RP (2010) Excitation of an upper hybrid wave by two intense laser beams and particle acceleration. *Physics Letters A* **374**, 866.

Rawat P, Gauniyal R and Purohit G (2014) Growth of ring ripple in a collisionless plasma in relativistic- ponderomotive regime and its effect on stimulated Raman backscattering process. *Physics of Plasmas* **21**, 06210.

Sharma RP and Singh RK (2013) Stimulated Brillouin backscattering of filamented hollow Gaussian beams. *Laser and Particle Beams* **31**, 689.

Sharma A and Kourakis I (2010) Spatial evolution of a *q*-Gaussian laser beam in relativistic plasma. *Laser and Particle Beams* **28**, 479.

Sharma RP, Vyas A and Singh RK (2013) Effect of laser beam filamentation on coexisting stimulated Raman and Brillouin scattering. *Physics of Plasmas* **20**, 102108.

Singh A and Walia K (2011*a*) Self-focusing of Gaussian laser beam in collisional plasma and its effect on second harmonic generation. *Laser and Particle Beams* **29**, 407.

Singh A and Walia K (2011*b*) Self-focusing of Gaussian laser beam through collisionless plasmas and its effect on second harmonic generation. *Journal of Fusion Energy* **30**, 555.

Singh A and Walia K (2013) Effect of self-focusing of Gaussian laser beam on second harmonic generation in relativistic plasma. *Journal of Fusion Energy* **33**, 83.

Sodha MS, Sharma S and Kaw PK (1968) Non-linear second harmonic generation in inhomogeneous semiconductors at low temperatures. *Journal of Physics C Solid State Physics* **1**, 1128.

Sodha MS, Sharma JK, Tewari DP, Sharma RP and Kaushik SC (1978) Plasma wave and second harmonic generation. *Plasma Physics* **20**, 825.

Stamper JA, Lehmberg RH, Schmitt A, Herbst MJ, Young FC, Gardner JH and Obenshain SP (1985) Evidence in the second-harmonic emission for self-focusing of a laser pulse in a plasma. *Physics of Fluids* **28**, 2563.

Tajima T and Dawson JM (1979) Laser electron accelerator. *Physical Review Letters* **43**, 267.

Teubner U and Gibbon P (2009) High-order harmonics from laser-irradiated plasma surfaces. *Reviews of Modern Physics* **81**, 445.

Volfbeyn P, Esarey E and Leemans WP (1999) Guiding of laser pulses in plasma channels created by the ignitor-heater technique. *Physics of Plasmas* **6**, 2269.

Wang L, Hong XR, Sun JN, Tang RA, Yang Y, Zhou WJ, Tian JM and Duan WS (2017) Effects of relativistic and channel focusing on *q*-Gaussian laser beam propagating in a preformed parabolic plasma channel. *Physics Letters A* **381**, 2065.

Yadav P, Gupta DN and Avinash K (2016) Suppression of stimulated Brillouin instability of a beat-wave of two lasers in multiple-ion-species plasmas. *Physics of Plasmas* **23**, 012110.

Young PE and Bolton PR (1996) Propagation of subpicosecond laser pulses through a fully ionized plasma. *Physical Review Letters* **77**, 4556.